Rhodamine B Discolouration on TiO_2 in the Cement Environment: A Look at Fundamental Aspects of the Self-cleaning Effect in Concretes

A. Folli[1], U. H. Jakobsen[2], G. L. Guerrini[3], and D. E. Macphee[1]

[1]Dept. of Chemistry, University of Aberdeen, Meston Walk, Aberdeen, AB24 3UE, UK
[2]Byggeri – Beton, DTI, Teknologisk Institut, Gregersensvej, Høje Tåstrup, Denmark
[3]CTG-Italcementi Group, Via Camozzi 124, Bergamo, 24121, Italy

Abstract:

The present work addresses the photocatalytic properties of two commercial titanias for application in concrete technology. A microsized, m-TiO_2 (average particle size 153.7 nm ± 48.1 nm) and a nanosized, n-TiO_2 (average particle size 18.4 nm ± 5.0 nm) have been tested. Cement paste samples (CEM I 52.5 cement, w/c=0.4) containing both photocatalysts have been evaluated based on Rhodamine B (RhB) discolouration under U.V. light, a standard test for self-cleaning cementitious materials. Experimental data are discussed in relation to photocatalyst properties (e.g.: particle size), dye adsorption and degradation characteristics. The influence of the chemical environment on photocatalyst performance and its impact on applications in construction concrete are also discussed.

Introduction

The photochemistry of TiO_2 has become a subject of intense research since Fujishima and Honda (1) and Wrighton et al. (2) reported the photocatalytic splitting of water on TiO_2 and Sr-doped TiO_2 respectively in the 1970s. Although TiO_2 has been known since 1929 to be responsible for the fading of colour in paints (3-4), it was only since the 1970s that TiO_2-based photo-catalysis has been widely applied as an advanced oxidation technology for environmental applications. Water and air remediation by oxidation, gas phase NO_x oxidation and solar cell applications have been amongst the most studied processes involving TiO_2 photo-chemistry as confirmed by the considerable number of publications, including several reviews (5-8), which have become available.

Applications of TiO_2 photocatalysts to construction materials began towards the end of the 1980s. Two important effects related to the nature of photoactive TiO_2 coatings had by this time been discovered: a) the self-cleaning effect due to redox reactions promoted by sunlight (or in general, weak U.V. light) on the photocatalyst surface (9), and b) the photo-induced hydrophilicity (10-11) of the catalyst surface, which enhances the self-cleaning effect (inorganics causing dirt and stains on surfaces can be easily removed due to rainwater soaking between the adsorbed substance and the TiO_2 surface). Photocatalytic glasses provide an example of self-cleaning and anti-fogging (wetting) properties, e.g. Pilkington Active™ (12). Recently, photocatalytic cementitious materials have been patented by Mitsubishi Corp.(NOxer™), and Italcementi SpA (TX-Aria™ and TX-Arca™), containing the TX-Active™ principle (13-18). The application of TiO_2 photocatalysis to concrete aims to achieve two main goals, the self-cleaning effect discussed above and the *depolluting* effect due to the oxidation of NO_x in the atmosphere to NO_3^-, especially in street canyons where NO_x concentrations can be considerable due to engine exhausts. The great advantage provided by such products is that the only requirements, beyond TiO_2 in the construction material used, are sunlight and rain-water.

Development of TiO_2 – cementitious binders providing self-cleaning has been carried out in order to enhance aesthetic durability of cementitious materials, particularly those based upon white cement. Although the use of such products is still restricted and limited, many buildings have been designed and constructed since 2000, to fulfil high aesthetic standards. Relevant examples are: Church "Dives in Misericordia", Rome, ITALY, Music and Arts City Hall, Chambéry, FRANCE, Police Central Station, Bordeaux, FRANCE, Air France Building, Roissy – Charles de Gaulle Airport, FRANCE, Saint John's Court, Montacarlo, MONACO.

In order to verify self-cleaning performances of photocatalytic cements/concretes, several tests involving organic substances have been set up mainly based upon the degradation of colour in dyes. Rhodamine B (*N-[9-(2-Carboxyphenyl)-6-diethylamino-3H-xanthen-3-ylidene]-N-ethyl-ethanaminium chloride*) is one of the most common dye tests and is adopted as an Italian standard (UNI 11259 (February 2008)). Rhodamine B (RhB) degradation on TiO_2 surfaces has been extensively studied in slurry systems (TiO_2 suspended in aqueous solutions of RhB) under different illumination conditions (19-23). Results have shown

 ISSN 1203-8407

efficient degradation of colour under both U.V. light and visible light. Under U.V. light illumination RhB is degraded by an ordinary *sensitised photoreaction* (5, 19) (a TiO_2 photocatalytic process involving photon absorption and electron promotion from the valence band, leaving positive holes, to the conduction band of the semiconductor, Figure 1(a)). Under visible light illumination, RhB undergoes a *dye-sensitisation* process, which is, effectively, a *catalysed photoreaction* (5, 19). The organic molecule absorbs visible light photons, which, whilst having insufficient energy to promote TiO_2 photo-activation, can promote electrons from the highest occupied molecular orbital (HOMO) to the lowest unoccupied molecular orbital (LUMO) in the organic molecule. These electrons are further injected from the RhB LUMO to the conduction band of TiO_2, leading to the formation of $RhB^{+\bullet}$ molecular ion radicals on the TiO_2 surface. The transfer of the conduction band electron to adsorbed oxygen on the TiO_2 surface produces $O_2^{-\bullet}$. Both radical species arising from this process are highly reactive leading ultimately to complete mineralization of the organic molecule (Figure 1(b)) (19-20).

Knowledge acquired from RhB degradation studies in aqueous TiO_2 slurry systems (19-23) has been extremely important in understanding degradation phenomena in other TiO_2-containing systems (solid surfaces). These insights into the surface chemistry of adsorption are more widely applicable and we consider here factors relevant to TiO_2 photocatalyst performance in cement systems.

Experimental and Methods

TiO_2 Samples – Throughout this study, two commercial available titanias: *m-TiO_2* (microsized) and *n-TiO_2* (nanosized), both 100% Anatase form, have been tested. Before starting any degradation experiments, these samples have been characterised in order to evaluate their main physical-chemical properties such as: light absorption characteristics, mineralogy, specific surface area, porosity and particle size. Light absorption measurements were undertaken to derive band-gap information and have been carried out on TiO_2 powders using U.V.-vis diffuse reflectance spectroscopy (StellarNet EPP2000 Spectrometer). Spectra were processed according to the Kubelka – Munk transform approach for indirect semiconductors as described in (24). X-Ray Diffraction patterns have been obtained using a Bruker D8 Advance diffractometer equipped with a $Cu_{K\alpha 1}$ 1.54Å X-Ray source operating at room temperature, in order to confirm the mineralogy and crystallinity. BET (Brunauer – Emmett – Teller (25)) specific surface area (S_{BET}) has been

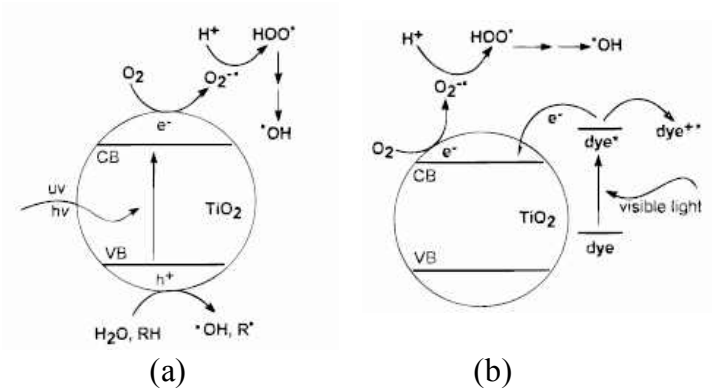

Figure 1. RhB-TiO_2 system: (a) U.V. light irradiation: *photo-sensitised* pathway; (b) visible light irradiation: *dye-sensitised* pathway (19).

obtained by N_2 adsorption on powder samples using a Micromeritics ASAP 2020. These data enabled characterisation of sample porosity as determined by the BJH (Barrett – Joyner – Halenda) model (26), assuming cylindrical pores. Samples were degassed at 150°C before adsorption measurements. Finally, particle size evaluation was carried out by three different techniques: TEM imaging (and further image analysis), XRD *via* the Scherrer equation (1) and a simple geometrical model derived from the BET specific surface areas assuming particles to be rigid spheres, equation (2);

$$d = \frac{0.9 \cdot \lambda}{FWHM \cdot \cos\theta_P} \quad (1)$$

$$d = \frac{6}{\rho_A \cdot S_{BET}} \quad (2)$$

where: in eq. (1), λ is the X-ray wavelength, FWHM, the full width at half maximum height for the Anatase 101 peak at 25.2° (2θ), θ_P, the Bragg's diffraction angle for the same peak and in eq. (2), ρ_A, the density of Anatase taken as 3.895 gcm^{-3}, and S_{BET}, the BET Specific Surface Area.

Cement Pastes Preparation – Two sets of photocatalytic cement pastes were prepared, one for each of the two commercial TiO_2 products. The TiO_2 and fresh white Portland cement (CEM I 52.5) powders were dry mixed in the mass ratio 3.5:96.5. 20g of the mixture was subsequently hydrated with 8g of distilled water (water:cement ratio, w/c=0.4). A third set (control) was prepared without photocatalyst. After mixing, pastes were cast in 42mm diameter moulds and cured for one day at room temperature and 80.5% relative humidity (over a saturated solution of $(NH_4)_2SO_4$). Six cement discs were produced for each set. The amount of titanium dioxide mixed with cement fulfils general criteria specified in Italcementi patents (13, 14, 16).

RhB Discolouration Experiments – After one day of curing, all samples were coated with 20µl of aqueous Rhodamine B solution (1g/l). The coating area was approximately 1.2cm^2. Three of the six discs per set were conditioned for 30 minutes under daylight, the remaining three were coated and conditioned for 30 minutes in darkness. All three sets were subsequently irradiated with a UVItec LI-208.m lamp (2 tubes 8W each, main wavelength 312nm) and reflectance measurements were performed after various illumination times using a StellarNet EPP2000 Spectrometer.

SEM Investigation on TiO_2 Dispersion in the Cement Matrix – A SEM investigation was performed in order to evaluate the dispersion effectiveness of TiO_2 in the cement system. The instrument used was a FEI Quanta 400 Scanning Electron Microscope equipped with a Thermo NSS-UPS-SEM-INORAN System SIX for X-ray microanalysis (EDS). Back-scattered electron images have been collected for the top surfaces (no impregnation, no coating, low vacuum mode) and across a section perpendicular to the surface (impregnation according to the method described in (27, 28)).

Results and Discussion

Physical Characterisation of Commercial Photocatalysts

The results of X-ray diffraction analyses are shown in Figure 2. The peak positions confirm that both commercial TiO_2 products are essentially Anatase (29, 30). Specific surface data are reported in Table 1. The much lower level of N_2 adsorption on the microsized sample is consistent with this sample showing larger crystallites than the nanosized product as expected, and indeed, the BJH analysis (Figure 3) shows that considerable agglomeration has occurred in the nano-sized sample under the conditions of testing, i.e. the pores arise from inter-particle volume. The corresponding porosity data cannot be obtained for the microsized sample as pore sizes are outside the measureable range.

Figure 4 shows transmission electron micrograph images of both products. Again the crystallite size difference between the two samples is evident and this is quantitatively supported by the histograms shown as insets in the figure. The above data are summarised in Table 1. In terms of particle size evaluation, there is good agreement between the techniques and the results are consistent with manufacturers' data.

Photocatalytic Performance

The degradation of colour of RhB was quantitatively measured by light absorption as a function of

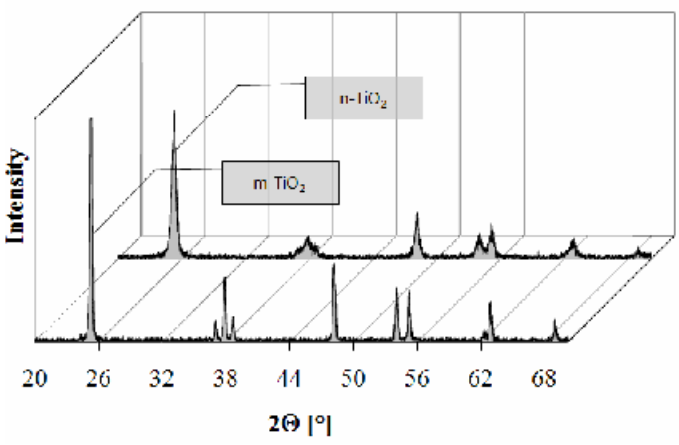

Figure 2. X-Ray diffraction patterns for both m-TiO_2 and n-TiO_2.

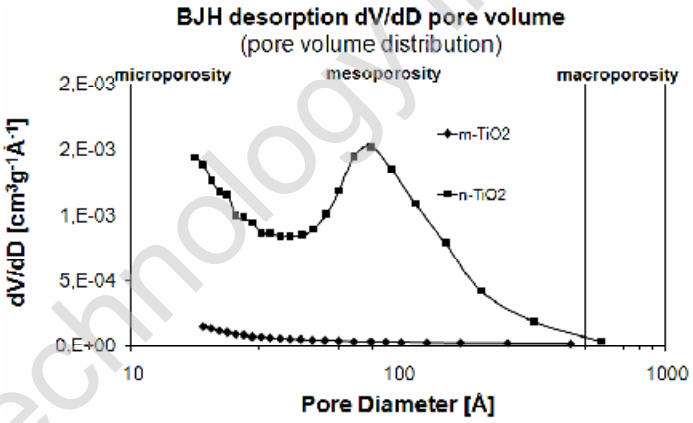

Figure 3. BJH plot for porosity evaluation.

wavelength. In the present study, the measurement of light absorption was obtained by reflecting light from the cement surface on which the dye is deposited. In this way, diffuse reflectance spectra are obtained as shown in Figure 5-7. The peak area of the main absorption centred around 541.5 nm is indicative of the concentration of the intact dye molecule and it can be observed that under illumination, the area reduces as a function of time, i.e. the dye molecule degrades. It can be noted that there is also degradation of colour in samples which do not contain photocatalyst and this highlights an important source of misrepresentation of catalyst efficiency where controls are not used. The loss of colour by photolytic degradation of the dye is quite common – in fact, this effect is observed as coloured fabrics are bleached in sunlight. However, even by taking account of this effect, it can be shown that there is an enhanced degradation of colour in the presence of photocatalyst.

An interesting feature of these data is the shift to lower wavelengths of absorption maxima exhibited by samples which experienced exposure to daylight during the dye deposition step. This feature is not reproduced when dye is deposited in the dark. A similar effect (hypsochromic shift) was observed by Chen *et al* (20),

Table 1. TiO_2 physical characterisation data ((a) particle mean count, (b) Gaussian interpolation from histograms).

Sample	Crystalline Phase	Band Gap	S_{BET}	BJH Φ_{pore}	Particle size			
					TEM (a)	TEM (b)	XRD	BET
		eV	m^2g^{-1}	*Å*	*nm*	*nm*	*nm*	*nm*
m-TiO_2	100% Anatase	3.29±0.02	8.7	Outside mesoporosity field	153.7±48.1	145.4±5.9	–	177.6
n-TiO_2	100% Anatase	3.34±0.02	78.9	79.6	18.4±5.0	18.2±0.5	16.6±2.0	19.5

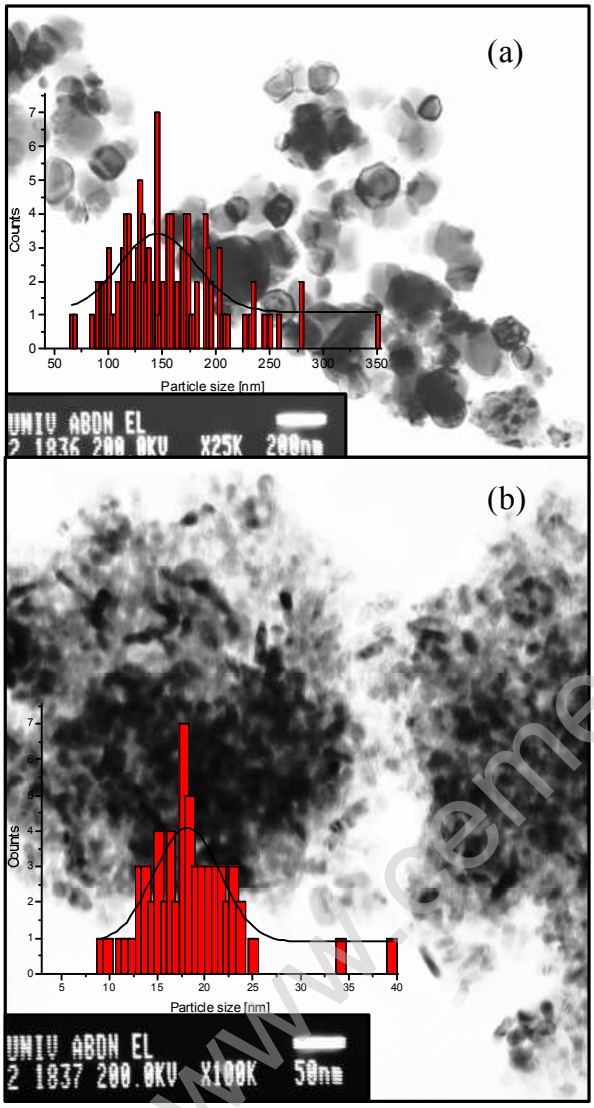

Figure 4. T.E.M. micrographs and particle size distribution of: (a) m-TiO_2, (b) n-TiO_2.

who discriminated between different degradation mechanisms as a function of the different illumination conditions experienced. The lower energies available from visible light are insufficient to induce photoactivation of TiO_2 but they can lead to dye sensitisation and degradation of colour by this mechanism. As a result, the selective stepwise de-ethylation of RhB amino groups (RhB adsorption on negatively charged TiO_2 surface), responsible for the hypsochromic shift, leads to a sequence of structurally similar degradation products which absorb radiation at progressively lower wavelengths. Where samples were prepared in the dark, the only light exposure was to UV radiation which promotes true photocatalytic processes, more aggressive oxidation due to the action of photo-generated holes and hydroxyl radicals, and reduces the hypsochromic effect.

Clearly, degradation mechanisms are important in understanding optimisation of photocatalyst efficiencies. However, it is evident from the above that photocatalysis can encompass more than one process. Whilst UV exposure promotes conventional photocatalysis-induced redox processes on the surface of TiO_2, diagnosis of reaction pathways is complicated by the dye sensitisation mechanism and the influence of resulting products. A further physical implication is the particle size of the photocatalyst. The dye sensitisation route would appear to be less dependent on the normally expected nano-dimensionality of the catalyst because charge recombination effects must be less significant, i.e. degradation is not dependent on the production of electron-hole pairs. It is therefore difficult to reconcile higher degradation rates for RhB on microsized TiO_2, with conventional photocatalytic mechanisms and the dominant effect under the conditions used in the study must therefore be dye sensitisation.

It is interesting to contrast the behaviour of the photocatalysts studied with different reducing agents. In the first stage of a gas phase study conducted on the oxidation of NO_x, we observed that in contrast to the experience with RhB, the nanosized TiO_2 seemed to perform better than the microsized TiO_2. Although these data are very preliminary, this observation highlights the complexity of interpreting data from photocatalytic studies. Of the different degradation mechanisms already mentioned, the conventional photocatalyst mechanism is the only one active for NO_x but, in assessing the oxidising potential of the different catalysts, other factors (such as the efficiencies of light absorption, charge transfer processes and adsorption) must be considered. If it is accepted that adsorption of the oxidisable species on the catalyst is the first step

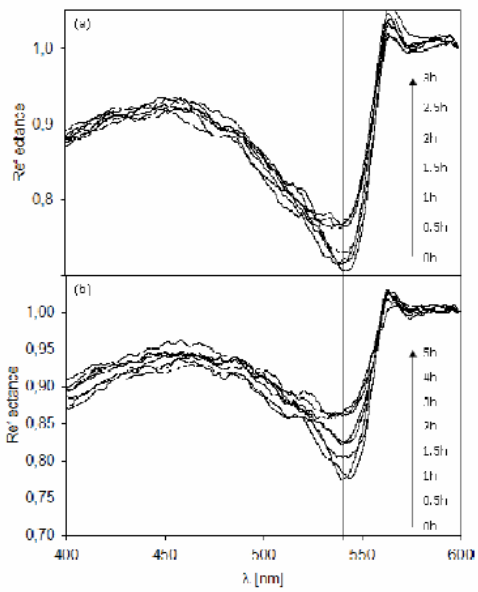

Figure 5. Diffuse reflectance spectra at various illumination time for white cement pastes without photocatalyst: (a) RhB deposition and conditioning under daylight, (b) RhB deposition and conditioning in darkness.

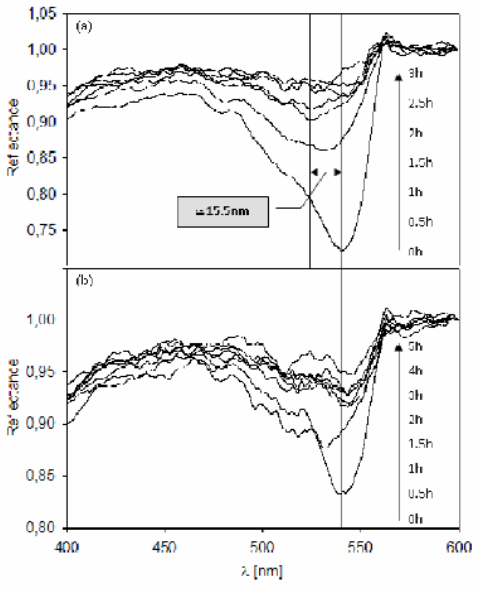

Figure 6. Diffuse reflectance spectra at various illumination time for white cement pastes containing m-TiO_2: (a) RhB deposition and conditioning under daylight, (b) RhB deposition and conditioning in darkness.

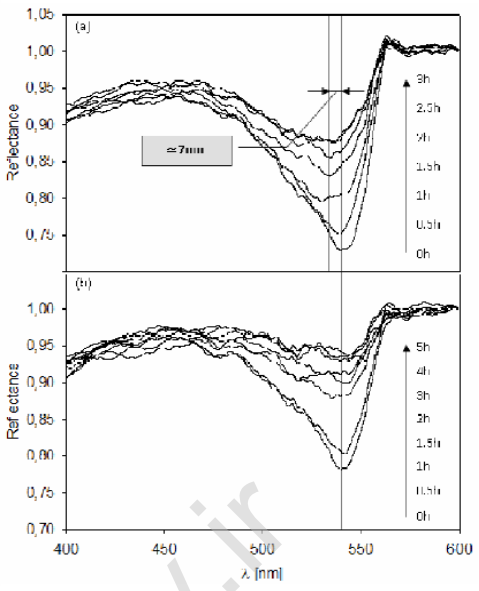

Figure 7. Diffuse reflectance spectra at various illumination time for white cement pastes containing n-TiO_2: (a) RhB deposition and conditioning under daylight, (b) RhB deposition and conditioning in darkness.

of degradation, it must then be important to consider how efficiently the adsorbate is adsorbed. To address this properly, one needs to consider the surface charges on the catalyst under the conditions of the experiment and the charges on the target molecule. In aqueous solution without complexing cations, the zeta potential of TiO_2 varies with pH according to Figure 8. Chen et al. (20) presented a detailed analysis of adsorption characteristics for RhB on TiO_2 which highlights the significance of surface charges to adsorption geometry. Of the two possible binding modes for RhB on TiO_2 (20), only binding *via* the amine groups the subsequent degradation leads to the observed hypsochromic shift (selective stepwise de-ethylation (20)). This suggests that surfaces on TiO_2 in this study are negative under these conditions. This is confirmed by the ionization of surface TiOH groups in an alkaline environment (39):

$$TiOH + OH^- \rightarrow TiO^- + H_2O \qquad (3)$$

Whilst surface charges dictate adsorption properties, they also have an important influence on the dispersion of the particles. Aggregation/dispersion behaviour of TiO_2 particles in the cement environment cannot be described by the DLVO (Derjaguin, Landau, Verwey, Overbeek) theory (31, 32) on stability of colloids. DLVO is applicable to systems where particles are weakly charged in monovalent electrolytes at low concentrations and is inappropriate for highly coupled systems characterised by high ionic strengths, high

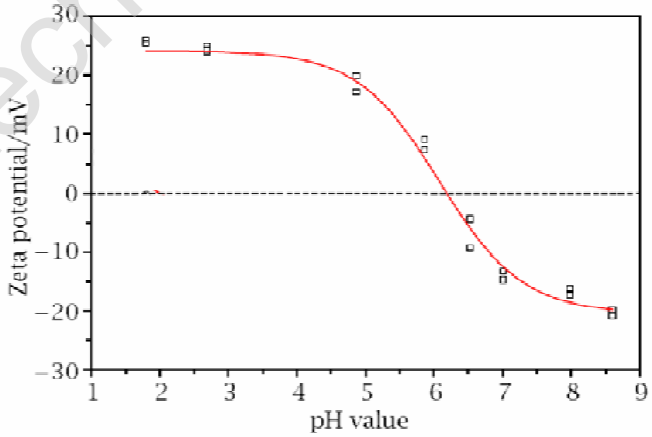

Figure 8. TiO_2 ζ-potential in aqueous solution without complexing cations (20).

surface charge densities and containing multivalent ions, which exhibit specific adsorption on particle surfaces. Indeed, the Poisson-Boltzmann equation supporting the DLVO theory doesn't take into account the ion-ion correlations between co- and counter- ions in the Electric Double Layer (EDL, Stern model), which can account for the attraction between particles with apparently the same charges. Such phenomena have been demonstrated by many authors working on different colloidal systems and have been confirmed by several simulations (33-39) as identified in two recent reviews (40, 41).

Attractive forces due to ion-ion correlations are expected at high surface charge densities. This is shown in detail by Mange et al. (39) for TiO_2 (Anatase)

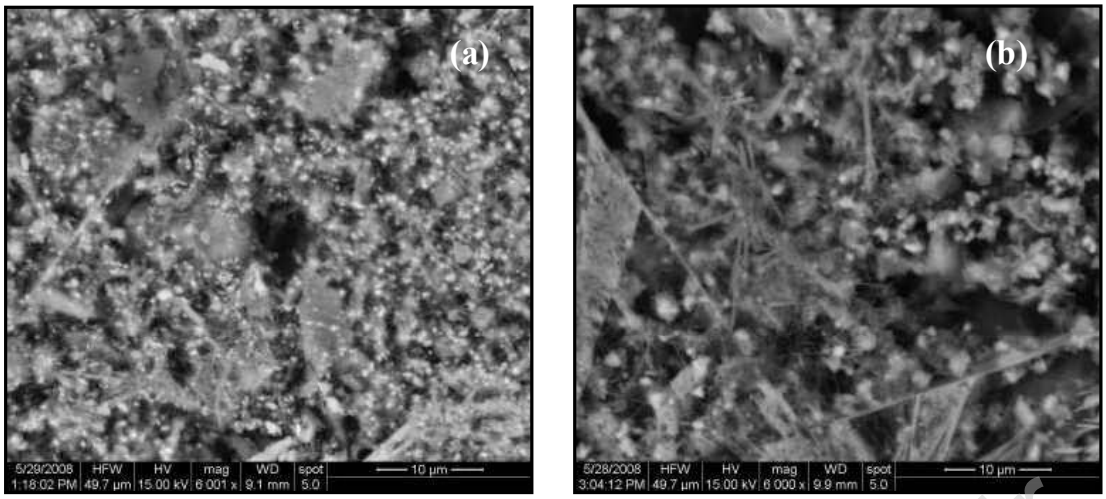

Figure 9. SEM surface micrographs for cement specimens (1 day cured) prepared with: (a) m-TiO_2, (b) n-TiO_2. SEM conditions adopted: no impregnation, no coating, low vacuum mode.

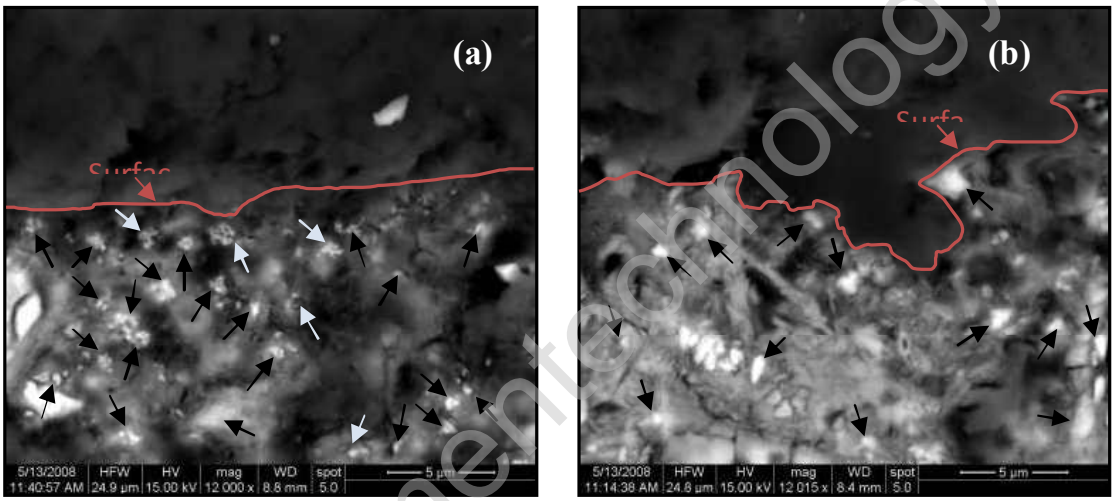

Figure 10. SEM polished cross section micrographs for cement specimens (1 day cured) prepared with: (a) m-TiO_2, (b) n-TiO_2. SEM conditions adopted: impregnation (27, 28), no coating, low vacuum mode.

suspensions at high pH in the presence of Ca^{2+} ions and by Jönsson et al. and Labbez et al. for C-S-H (calcium – silica hydrates) particles in hydrated cement. Furthermore, surface charge density is highly particle size-dependent. Abbas et al. showed for a fixed electrolyte concentration that, according to the corrected Debye-Hückel theory of surface complexation, the smaller the particles, the higher their surface charge density due to an improved screening efficiency of the counter- ions as the particle surface becomes increasingly curved (42). This effect, confirmed by Monte-Carlo simulations, is extremely enhanced below a particle diameter of 10 nm. The same authors have also shown that the surface charge density increases with the electrolyte equilibrium concentration.

From the considerations above, a higher surface charge density for the n-TiO_2 in the high ionic strength environment of cement should therefore be expected. This would lead to a stronger ion-ion correlation effect, between the negatively charged TiO_2 surfaces and the associated aqueous Ca^{2+} ions, and, ultimately, a higher degree of agglomeration. Further, it is known that aggregation also depends on the number of particles in the system. If we approximate TiO_2 particles to perfect spheres, from a simple geometric calculation we can derive that for a given mass of TiO_2, the total number of particles for the n-TiO_2 is 9^3 times the one for the m-TiO_2, also suggesting a higher degree of agglomeration in the n-TiO_2.

An SEM survey on the hardened cement samples has been carried out to evaluate the dispersion effectiveness of the two titanias in the cement environment. Micrographs in Figure 9 were obtained for the surface layer of the cement samples prepared with m-TiO_2 (Figure 9(a)) and n-TiO_2 (Figure 9(b)) whilst micrographs in Figure 10 are of sections cut perpendicularly to the surface and show the layers beneath the surface. Surface micrographs (Figure 9) show a higher degree of m-TiO_2 dispersion (white spots in Figure 9(a)). Cement prepared with nanosized n-TiO_2 show larger

particle aggregates (a lower degree of dispersion (see Figure 9(b))). This is especially evident when the scale of the micrograph is considered. Nanoparticulate agglomerates seem to be at least 1 μm in dimension compared to m-TiO_2 agglomerates which seem to be smaller and divided in smaller sub-agglomerates. A very similar situation is achieved in the bulk of the specimens, see Figure 10. Figure 10(a), related to cement prepared with m-TiO_2, shows smaller and better dispersed TiO_2 particle aggregates compared with n-TiO_2-containing pastes, Figure 10(b). This evidence seems to be in good agreement with the simulations by Abbas et al. and the hypothesis derived from the expected surface charge density and ion-ion correlations. Whilst it should also be considered that the commercial titanias may already be agglomerated prior to introduction to the cement, the considerations above offer some explanation as to the different degrees of agglomeration that could be expected (and are observed) as a consequence of the cement environment. Electrokinetic measurements are currently being performed to quantify actual surface charges and ζ-potential trends. Beyond understanding the different dispersion characteristics of TiO_2 in the cement environment, these parameters can also be useful to interpret the adsorption chemistry of RhB (or other charged molecules) on TiO_2 in cement/concrete systems, particularly where adsorbed Ca^{2+} ions compete to form the electric double layer. The selective de-ethylation (hypsochromic shift (20)) observed for TiO_2 exposed to daylight (Figure 6-7 (a)) suggests that RhB is bound to the catalyst *via* its amino groups (partial positive charge), indicating that the surface is negatively charged. This is consistent with the arguments presented on dispersion. The difference in performance between m-TiO_2 and n-TiO_2 is therefore considered to be a consequence of surface charge density. It is tentatively proposed that the higher negative surface charge on n-TiO_2 is more readily satisfied by Ca^{2+} adsorption, reducing the binding of RhB whereas, Ca^{2+} is less strongly associated with m-TiO_2 and RhB binding is quantitatively more significant leading to higher rates of degradation *via* dye sensitisation.

Conclusions

A series of RhB dye discolouration studies have been undertaken using two commercial TiO_2 samples of different particle size distributions (predominantly microsized – 150 nm and nanosized – 18 nm), dispersed in white Portland cement. Differences in dye discolouration characteristics were observed for the microsized catalyst depending on whether or not the sample was exposed to visible light. Only a small effect was observed for samples containing the nanosized catalyst. Samples containing microsized TiO_2 experiencing visible light exposure showed evidence of selective de-ethylation through a dye-sensitisation mechanism (hypsochromic shift (20)) leading to a different dye degradation pathway to that taken by exposure to UV only. The observation from photocatalytic tests that microsized titania shows a higher RhB discolouration performance than nanosized titania in the cement environment is likely to be associated with either a higher degree of dispersion, observed by SEM, and the higher exposed surface area for dye adsorption, or more fundamental surface chemistry, which is being addressed in a subsequent paper.

Acknowledgments

The authors are grateful to the European Community under the Marie Curie Research Training Network MRTN-CT-2005-019283" Fundamental understanding of cementitious materials for improved chemical physical and aesthetic performance" (http://www.nanocem.org/MC-RTN/) for the full support of Andrea Folli.

The authors are also grateful to Prof. A. Nonat, Dr. C. Labbez and Dr. I. Pochard (Université de Bourgogne, Dijon Cedex, FRANCE) for the helpful discussions about stability of TiO_2 colloidal suspensions in highly coupled systems.

References

(1) Fujishima, A.; Honda, K. *Nature* **1972**, *238*, 37-38.

(2) Wrighton, M.S.; Ellis, A.B.; Wolczanski, P.T.; Morse, D.L.; Abrahamson, H.B; Ginley, D.S. *J. Amer. Chem. Soc*. **1976**, *98*, 2774. P.T.

(3) Keidel, E. *Furben Zeitung* **1929**, *34*, 1242.

(4) Goodeve, C.F.; Kitchner, J.A. *Trans. Farad. Soc*. **1938**, *34*, 570.

(5) Mills, A.; Le Hunte, S. *J. Photochem. and Photobiol. A: Chemistry* **1997**, *108*, 1-35.

(6) Legrini, O.; Oliveros, E.; Braun, A.M. *Chem. Rev.* **1993**, *93*, 671-698.

(7) Ollis, D.; Al-Ekabi, H. *Photocatalytic purification and treatment of water and air*, Elsevier, NY 1993.

(8) Ryu, J. ; Choi, W. *Environ. Sci. Tech*. **2008**, *42*, 294-300.

(9) Fujishima, A.; Hashimoto, K.; Watanabe, T. *TiO_2 photocatalysis: Fundamentals and Applications*, BKC Tokyo, 1999.

(10) Wang, R.; Hashimoto, K.; Fujishima, A.; Chikuni, M.; Kojima, E.; Kitamura, K.; Shimohigoshi, M.; Watanabe, T. *Nature*, **1997**, *338*, 431-432.

(11) Irie, H.; Siew-Ping, T.; Shibota, T.; Hashimoto, K. *Electrochem. Solid State Lett*. **2005**, *8*, 23-25.

(12) Patent Application WO 98/06675.

(13) Italcementi SpA, US 6409821.

(14) Italcementi SpA, WO 2006/565.

(15) EP Patent 0786283 A1, Mitsubishi Corp.

(16) EP Patent 1601626, Italcementi SpA.

(17) Cassar, L.; Beeldens, A.; Pimpinelli, N.; Guerrini, G.L. *International RILEM Symposium on Photocatalysis, Environment and Construction Materials Proceedings*; 2007, pp 131-145.

(18) Guerrini, G.L.; Plassais, A.; Pepe, C.; Cassar, L. *International RILEM Symposium on Photocatalysis, Environment and Construction Materials Proceedings*, 2007, pp 219-226.

(19) Wu, T.; Liu, G.; Zhao, J.; Hidaka, H.; Serpone, N. *J. Phys. Chem. B*. **1998**, *102*, 5845-5851.

(20) Chen, F.; Zhao, J.; Hidaka, H. *Intern. J. Photoenergy* **2003**, *05*, 209-217.

(21) Soares, E.T.; Lausarin, M.A.; Moro, C.C. *Brazilian J. Chem. Engineering* **2007**, *24*, 29-36.

(22) Li, J.; Ma, W.; Lei, P.; Zhao, J. *J. Envir. Sciences* **2007**, *19*, 892-896.

(23) Li, J.; Li, L.; Zheng, L.; Xian, Y.; Jin, L. *Electrochimica Acta* **2006**, *51*, 4942-4949.

(24) Lin, H.; Huang, C.P.; Li, W.; Ni, C.; Ismatshah, S.; Tseng, Y. *Appl. Cat. B: Environmental* **2006**, *68*, 1-11.

(25) Brunauer, S.; Emmett, P.H.; Teller, E. *J. Amer. Chem. Soc.* **1938**, *60*, 309-319.

(26) Barrett, E.P.; Joyner, L.G.; Halenda, P.P. *J. Amer. Chem. Soc.* **1951**, *73*, 373-380.

(27) Jakobsen, U.H.; Laugesen, L.; Thaulow, N. *Determination of water to cement ratio in hardened concrete by optical fluorescence microscopy. ACI Symposium Volume: Water-Cement ratio and other Durability Parameters: Techniques for determination*. SP 191, 2000.

(28) Jakobsen, U.H.; Brown, D.R.; Comeau, R.J.; J.H.H. Henriksen *Eurosem* 2003.

(29) Bruker EVA X-ray diffraction pattern database.

(30) ATOMS Software.

(31) Derjaguin, B.V. ; Landau, L.P. *Acta Phys. Chim. USSR* **1941**, *14*, 633.

(32) Verwey, E.J.W.; Th. J.; Overbeek, G. *Theory and stability of lyophobic colloids*; Elsevier, Amsterdam: 1948.

(33) Guldbrand, L.; Jönsson, B.; Wennerström, H.; Linse, P. *J. Chem. Phys*. **1984**, *80*, 2221.

(34) Wennerström, H.; Jönsson, B. *J. Phys. France* **1988**, *49*, 1033.

(35) Jönsson, B.; Nonat, A.; Labbez, C.; Cabane, B.; Wennerström, H. *Langmuir* **2005**, *21*, 9211-9221

(36) Labbez, C.; Jönsson, B.; Pochard, I.; Nonat, A.; Cabane, B. *J. Phys. Chem*. **2006**, *110*, 9219-9230.

(37) Valleau, J.P.; Ivkov, R.; Torrie, G.M. *J. Chem. Phys.* **1991**, *95*, 520.

(38) Tang, Z.; Scriven, L.E.; Davis, H.T. *J. Chem. Phys*. **1992**, *97*, 9258.

(39) Mange, F.; Couchot, P.; Foissy, A.; Pierre, A. *J. of Colloid and Interface Sci*. **1993**, *159*, 58-67.

(40) Attard, P. *Adv. Chem. Phys*. **1996**, *92*, 1.

(41) Quesada-Perez, M.; Gonzalez-Tovar, E.; Martin-Molina, A.; Lozada-Cassou, M.; Hidalgo-Alvarez, R. *ChemPhysChem* **2003**, *4*, 235.

(42) Abbas, Z.; Labbez, C.; Nordholm, S.; Ahlberg, E. *J. Phys. Chem. C*. **2008**, *112*, 5715-5723.

Received for review September 22, 2008. Accepted December 18, 2008.